

Size-Dependent Electron Injection from Excited CdSe Quantum Dots into TiO₂ Nanoparticles

István Robel,^{†,¶} Masaru Kuno,^{*,†,‡} and Prashant V. Kamat^{*,†,§}

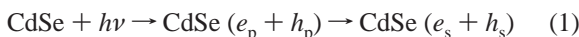
Radiation Laboratory, Department of Chemistry and Biochemistry, Department of Chemical and Biomolecular Engineering, and Department of Physics, University of Notre Dame, Notre Dame, Indiana 46556

Received January 5, 2007; E-mail: pkamat@nd.edu

Semiconductor quantum dots such as CdSe, PbSe, and InAs with their tunable band gaps offer new opportunities for harvesting light energy in the visible and infrared regions of solar light.^{1–3} Early efforts demonstrated the ability of chemically and electrochemically deposited CdS and CdSe nanostructures on TiO₂,^{4–6} SnO₂,^{7,8} and ZnO^{9,10} to generate photocurrent under visible light irradiation. By making use of size quantization effects, one can readily tune the photoresponse of the electrode. We report here modulation of the interparticle electron transfer rate by varying the QD particle size. Femtosecond transient absorption measurements, elucidating the size-dependent electron injection rate from excited CdSe into TiO₂ nanoparticles, are described.

Figure 1A shows the absorption spectra of different sized CdSe particles in toluene. These particles prepared using a previously reported procedure^{11,12} exhibit absorption in the visible with a characteristic exciton absorption peak. By comparing the absorption behavior to the size-dependent absorption curve,¹³ we estimated the particle diameter for five different size particles. As the particle size decreases from 7.5 to 2.4 nm, the first (1S_{3/2}1S_s) excitonic peak shifts (Figure 1A) from 645 nm (1.92 eV) to 509 nm (2.44 eV). Controlling particle size therefore provides a convenient way to modulate the band energies and the energy of the charge carriers.

The CdSe nanoparticle suspensions, when subjected to the 387 nm pump pulse, undergo photoexcitation followed by relaxation to band edge states (reaction 1).



As the electrons and holes accumulate in the conduction and valence bands, one observes bleach in the absorption. Figure 1B shows the difference absorption spectra of different size CdSe quantum dots in the visible region recorded 2 ps after 387 nm pulse excitation. The bleaching maximum of each of these different size CdSe quantum dots coincides with the first exciton transition seen in the absorption spectrum (Figure 1A). As shown earlier, excitation with the 387 nm laser pulse populates the higher energy p-state within the laser pulse duration, which then relaxes to the lower s-state in <1 ps.^{14,15} Thus, the bleaching at the band edge seen in the transient absorption in Figure 1B provides a means to probe the fate of electrons accumulated in the thermally relaxed s-state.

The recovery of the transient bleach (depletion of absorption) in Figure 1B represents the disappearance of the photogenerated electrons and holes via charge recombination and charge trapping processes.^{16–18} As shown by spectroelectrochemical measurements, the absorption bleach at the band edge is dominated by the presence of the electrons in the conduction band,¹⁹ while holes have

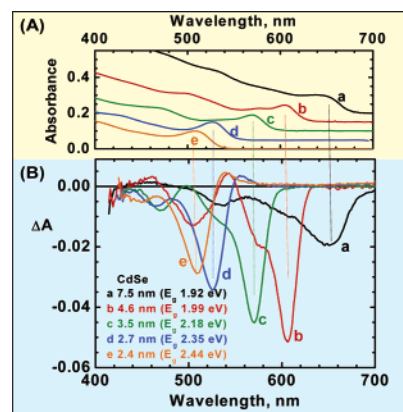


Figure 1. (A) Absorbance spectra of CdSe quantum dots in toluene. (Y-axis offset is introduced for clarity.) (B) Transient absorption spectra recorded 2 ps following the 387 nm laser pulse excitation of different size CdSe quantum dots in 1:1 ethanol/tetrahydrofuran (THF).

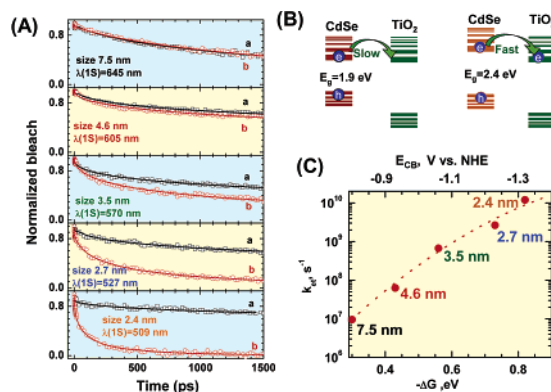


Figure 2. (A) The transient recovery recorded at the bleaching maximum following 387 nm laser pulse excitation of CdSe quantum dots in 1:1 ethanol/THF containing mercaptopropionic acid (a) without and (b) with linked TiO₂ particles. (B) Scheme illustrating the principle of electron transfer from quantized CdSe into TiO₂ and (C) the dependence of electron transfer rate constant on the energy difference between the conduction bands. Top axis represents assumed CdSe conduction band energy positions.

negligible contribution. The multiexponential nature of the recovery arises from the combination of radiative and nonradiative (trapping) processes. As shown earlier, the bleaching recovery is sensitive to the degree of surface passivation.¹⁵ The bleaching recoveries for different size particles (Figure 2) were analyzed using the stretched exponential kinetic expression:

$$\Delta A(t) = \Delta A(0) \times \exp[-(t/\tau)^\beta] \quad (2)$$

where τ is the peak value of the characteristic lifetime. Such a universal stretched exponential behavior has been previously observed in the carrier relaxation dynamics of various photoexcited

[†] Radiation Laboratory.

[‡] Department of Chemistry and Biochemistry.

[§] Department of Chemical and Biomolecular Engineering.

[¶] Department of Physics.

semiconductor nanocrystals.^{20–22} Kinetic parameters of the fits are summarized in Table S1. Except for the largest particle, the β value remained in the 0.4–0.5 range, consistent with previous time-resolved spectroscopic measurements of CdSe nanocrystals at room temperature.²¹

When in contact, the excited CdSe quantum dots are capable of injecting electrons into TiO₂ nanoparticles.^{3,23} The TiO₂ particle has a band gap of ~ 3.4 eV, exhibiting absorption in the UV region with onset around 360 nm. The TiO₂ particles prepared by the hydrolysis of titanium isopropoxide in ethanol are relatively large³ (particle diameter 40–50 nm) compared to the CdSe QDs. Such large particle surface enables linking of several small CdSe particles to a single TiO₂ particle and facilitates interparticle electron transfer. We employed mercaptopropionic acid to link these two particles (see Supporting Information for experimental procedures). For 7.5 nm diameter CdSe colloids, the conduction band is estimated to be -0.8 versus NHE.¹⁹ The same study demonstrated that the conduction band shifts to negative potentials with decreasing particle size (e.g., -1.57 vs NHE for 3.0 nm particles). Because of the small electron effective mass ($m_e = 0.13 m_0$) versus the significantly larger hole mass ($m_h = 1.14 m_0$), most of the band gap increase is seen as a shift in the conduction band to more negative potentials (vs NHE).¹⁴ Thus, CdSe quantum dots with their increased band gaps are expected to have favorable conduction band energies for injecting electrons into TiO₂ (reaction 3).



The effect of the TiO₂ interaction with excited CdSe quantum dots is seen from the bleaching recovery recorded in Figure 2A. With decreasing particle size, we see an enhanced recovery suggesting an alternate deactivation pathway for the charges separated in CdSe. If electron transfer to TiO₂ is the only additional deactivation pathway for the excited-state interaction between CdSe and TiO₂ (reaction 3), we can estimate the rate constant (see Supporting Information) by comparing the bleaching recovery lifetimes in the presence and absence of TiO₂ (expression 4).

$$k_{\text{et}} = 1/\tau_{(\text{CdSe}+\text{TiO}_2)} - 1/\tau_{(\text{CdSe})} \quad (4)$$

Electron transfer kinetics in dye-sensitized SnO₂ and TiO₂ systems has been evaluated in terms of Marcus theory,^{24,25} for a nonadiabatic reaction in the classical activation limit. The theory implies that the logarithm of the electron transfer rate is a quadratic function with respect to the driving force, $-\Delta G$. This expression has been successfully applied by Hupp²⁶ and others²⁷ to investigate charge recombination kinetics in dye-sensitized SnO₂ and TiO₂. As the driving force, $-\Delta G$ (viz., energy difference between the acceptor and donor systems) increases, the rate of ET increases, reaching a maximum when the driving force equals the reorganization energy (i.e., when the activation free energy, $\Delta G^* = 0$).

In the present experiments, the driving force for the electron transfer between CdSe and TiO₂ is dictated by the energy difference between the conduction band energies. The conduction band of TiO₂ is at -0.5 V versus NHE.²⁷ If we assume the larger CdSe particles have band energy close to the reported value of -0.8 V versus NHE,¹⁹ we can use the increase in band gap as the increase in driving force ($-\Delta G$) for the electron transfer. Since the shift in the conduction band energy is significantly greater than the shift in valence band energy for quantized particles,¹⁴ we can expect the conduction band of CdSe QDs to become more negative (on NHE scale) with decreasing particle size. Figure 2C shows the energy gap dependence of $\log(k_{\text{et}})$. As the particle size decreases,

we see an enhanced electron transfer rate. The driving force of 0.8 eV is at or close to the reorganization energy, and hence we expect a normal Marcus region in which the rate of electron transfer increases with the driving force. This small energy difference attained by decreasing particle size is sufficient to increase the electron transfer rate by nearly 3 orders of magnitude.

The fastest electron transfer in the CdSe–TiO₂ system was observed with 2.4 nm CdSe QDs. The rate constant of $\sim 1.2 \times 10^{10} \text{ s}^{-1}$ in this experiment reflects an average lifetime of 83 ps. Earlier femtosecond transient studies have reported similar electron transfer rates between excited CdS/CdSe QDs and TiO₂ which occur on a time scale of 2–50 ps. Direct chemical deposition of CdS/CdSe on TiO₂ films in those studies²⁷ provided minimal control over their size distribution. To the best of our knowledge, the present study highlights for the first time systematic evaluation of size-dependent electron transfer rates in semiconductor heterostructures.

Size-dependent electronic properties of semiconductor QDs are regarded as one of the most attractive features for attaining a band gap gradient in quantum dot solar cells. The transient absorption measurements presented in this study demonstrate the possibility of modulating the electron transfer rate between CdSe and TiO₂ particles by making use of size quantization effects. These size-dependent interparticle electron transfer rates will have to be taken into account in band gap engineering efforts of quantum dot sensitized solar cells.

Acknowledgment. The research described herein was supported by the Office of Basic Energy Sciences of the U.S. Department of Energy. This is contribution NDRL 4707 from the Notre Dame Radiation Laboratory.

Supporting Information Available: Synthesis and procedures, table of kinetic analysis, and additional references. This material is available free of charge via the Internet at <http://pubs.acs.org>.

References

- (1) (a) Nozik, A. J. *Physica E* **2002**, *14*, 115. (b) Kamat, P. V. *J. Phys. Chem. C* **2007**, *111*, 2834.
- (2) Wang, Z. L. *J. Phys. Chem. B* **2000**, *104*, 1153.
- (3) Robel, I.; Subramanian, V.; Kuno, M.; Kamat, P. V. *J. Am. Chem. Soc.* **2006**, *128*, 2385.
- (4) Gerischer, H.; Luebke, M. *J. Electroanal. Chem.* **1986**, *204*, 225.
- (5) Spanhel, L.; Weller, H.; Henglein, A. *J. Am. Chem. Soc.* **1987**, *109*, 6632.
- (6) Hao, E.; Yang, B.; Zhang, J.; Zhang, X.; Sun, J.; Shen, J. *J. Mater. Chem.* **1999**, *8*, 1327.
- (7) Nasr, C.; Kamat, P. V.; Hotchandani, S. *J. Electroanal. Chem.* **1997**, *420*, 201.
- (8) Nasr, C.; Hotchandani, S.; Kim, W. Y.; Schmehl, R. H.; Kamat, P. V. *J. Phys. Chem. B* **1997**, *101*, 7480.
- (9) Hotchandani, S.; Kamat, P. V. *Chem. Phys. Lett.* **1992**, *191*, 320.
- (10) Hotchandani, S.; Kamat, P. V. *J. Phys. Chem.* **1992**, *96*, 6834.
- (11) Peng, Z. A.; Peng, X. *J. Am. Chem. Soc.* **2001**, *123*, 1389.
- (12) Yu, W. W.; Qu, L. H.; Guo, W. Z.; Peng, X. G. *Chem. Mater.* **2004**, *16*, 560.
- (13) Yu, W. W.; Qu, L. H.; Guo, W. Z.; Peng, X. G. *Chem. Mater.* **2003**, *15*, 2854.
- (14) Norris, D. J.; Bawendi, M. G. *Phys. Rev. B* **1996**, *53*, 16338.
- (15) Klimov, V. I.; McBranch, D. W. *Phys. Rev. Lett.* **1998**, *80*, 4028.
- (16) Burda, C.; Green, T. C.; Link, S.; El-Sayed, M. A. *J. Phys. Chem. B* **1999**, *103*, 1783.
- (17) Mohamed, M. B.; Burda, C.; El-Sayed, M. A. *Nano Lett.* **2001**, *1*, 589.
- (18) Klimov, V. I. *J. Phys. Chem. B* **2000**, *104*, 6112.
- (19) Wang, C. J.; Shim, M.; Guyot-Sionnest, P. *Science* **2001**, *291*, 2390.
- (20) Linnros, J.; Lalic, N.; Galeckas, A.; Grivickas, V. *J. Appl. Phys.* **1999**, *86*, 6128.
- (21) Beadie, G.; Sauvain, E.; Gomes, A. S. L.; Lawandy, N. M. *Phys. Rev. B* **1995**, *51*, 2180.
- (22) Phillips, J. C. *Rep. Prog. Phys.* **1996**, *59*, 1133.
- (23) Yu, P.; Zhu, K.; Norman, A. G.; Ferrere, S.; Frank, A. J.; Nozik, A. J. *J. Phys. Chem. B* **2006**, *110*, 25455.
- (24) Marcus, R. A.; Sutin, N. *Biochim. Biophys. Acta* **1985**, *811*, 265.
- (25) Marcus, R. A. *J. Chem. Phys.* **1965**, *43*, 679.
- (26) Gaal, D. A.; Hupp, J. T. *J. Am. Chem. Soc.* **2000**, *122*, 10956.
- (27) See Supporting Information for additional references.

JA070099A